Research Signpost
37/661 (2), Fort P.O., Trivandrum-695 023, Kerala, India

Nanoscale Interactions and their applications: Essays in honour of Ian McCarthy, (2006): 000-000 ISBN: 00-0000-000-0

Electron Momentum Spectroscopy of Crystals: from dream to reality

Maarten Vos
Atomic and Molecular Physics Laboratories, Research School of Physical Sciences and Engineering, Australian National University, Canberra, ACT, 0200 Australia

Abstract

The use of Electron Momentum Spectroscopy for the study of thin, single-crystal films is sketched. These films have an anisotropic electronic structure. Resolving this anisotropy in (e,2e) experiments has been a dream that has become a reality in recent years. Here I describe some results for graphite, silicon and noble metals. The experimental results are used to illustrate the concepts of Brillouin zone boundaries and Bloch functions, both central to condensed matter physics.

Correspondence/Reprint request: Dr. M. Vos , Atomic and Molecular Physics Laboratories, Research School of Physical Sciences and Engineering, Australian National University, Canberra, ACT, 0200 Australia E-mail: Maarten.Vos@anu.edu.au

Introduction

High energy scattering is an important probe of many-body systems. For high-energy, large angle scattering the probing particle interacts with a single particle of the many-body system and the collision appears to be between two free particles. In this high energy limit the energy lost by the scattered particle is entirely determined by the laws of energy and momentum conservation. The energy transferred from the scattered particle to the target in these so called Compton experiments depends on a specific momentum component of the scatterer (before the collision) and its mass. Thus although the collision appears to be between two free particles, the energy transfer depends on the initial momentum and, because of this, the scattering experiment is a probe for an interacting many-body system. Compton type experiments can be used to probe the wave function of nucleons inside a nucleus, the wave function of electrons in atoms, molecules and solids, and even the wave function of nuclei in molecules and solids [1].

If in these collisions enough energy is transferred to the scatterer, then it will be ejected from the system. Now experiments can be done at a new level of sophistication, by measuring the ejected and scattered particles *in coincidence*. These coincidence experiments have been done for incoming protons scattering from protons inside a nucleus and ejecting a proton (so called *(p,2p)* experiments see e.g. [2]) and incoming electrons scattering from electrons in atoms, molecules, or solid (so called *(e,2e)* experiments, also referred to as electron momentum spectroscopy (EMS) [3]). Measurement of the momentum and energy of the scattered and ejected particles (in coincidence) allows for the determination of the momentum transfer to the target, as well as the binding energy of the ejected particle. The observed intensity is proportional to the spectral function, or within an independent particle model, the probability that a target particle has momentum $\mathbf{q}$ and binding energy E. Often the target (nuclei, molecules) does not have spherical symmetry and is randomly oriented in space. The measurement obtains, in such a case, the spherically-averaged spectral function, and a great deal of information is lost in this averaging process. A more stringent test of theory would be possible if this averaging could be avoided. For *(e,2e)* experiments of molecules there are attempts being made to recover this information for the special case where the molecule fragments as a consequence of the ionization event [4]. Measuring the direction of the velocity of the fragments can reveal the original orientation of the molecule.

For *(e,2e)* experiments from solids one can completely avoid this problem by studying single crystals with known orientation. This is an important motivation for the study of these targets, and the significance of these measurements were realized in the early days of *(e,2e)* spectroscopy, see e.g.

the paper by Neudachim *et al* [5]. However the experiment turned out to be challenging. It requires good energy resolution to resolve the valence band structure, and high energies of the incoming and outgoing particles. Only when high energies for the incoming and outgoing particles are used (10 keV and above), and the thinnest of films, is the probability reasonably high that no scattering occurs, besides the *(e,2e)* event itself. Hence it was not until 1988 that Ritter and coworkers succeeded in measuring a single crystal (graphite) with a meaningful, but modest, resolution [6]. Since that time there have been significant improvements in the experimental capabilities, in particular the development of two-dimensional detectors [7], and nowadays single crystal measurements are done quite routinely (provided sufficiently thin crystals are available). In this contribution I want to show some examples of these measurements and emphasize that these measurements provide insightful illustrations of fundamental condensed matter concepts such as Brillouin zone boundaries and Bloch functions.

Mainly to keep the language simple I have adopted the independent particle picture in this paper. The target wave function is the product of single particle wave functions $\psi_i(\mathbf{r})$) (i=1…n). The momentum space representation of these orbitals is $\varphi_i(\mathbf{q})$ and $|\varphi_i(\mathbf{q})|^2$ is then the probability that electron i had momentum **q**.

Experimental Results

The experimental apparatus used at the Australian National University is described extensively elsewhere [8]. It is sketched in figure 1, together with the coordinate system used. It has two analyzers, each measuring simultaneously electrons emerging from the sample along a range of azimuthal angles (±7°) and over a range of energies (ΔE=60 eV). It uses an incoming electron beam of 50 keV and both analysers detect electrons with an energy near 25 keV. The z-axis is taken along the direction of the incoming electrons. The azimuthal range of one analyzer is centered at ϕ_1=0°, the other at ϕ_2=180°.The exact polar scattering angle $\theta_{1,2}$ can be adjusted using two deflector sets. If one applies no voltage to the deflectors then the scattering angles are θ_1=θ_2=44.3°, which means that for 50 keV electrons: $k_1\cos\theta_1 + k_2\cos\theta_2 = k_0$, and $k_1\sin\theta_1\cos\phi_1 \approx -k_2\sin\theta_2\cos\phi_2$. In this case one can thus expect coincidences originating from target electrons with no momentum component in the p_x-p_z plane. Their momentum component along the p_y-axis is: $q_y = k_1\sin\theta_1\sin\phi_1 + k_2\sin\theta_2\sin\phi_2$. The analysers determine ϕ_1 and ϕ_2. If one applies deflector voltages in such a way such that $\theta_1 = \theta_2 < 44.3°$ then one still

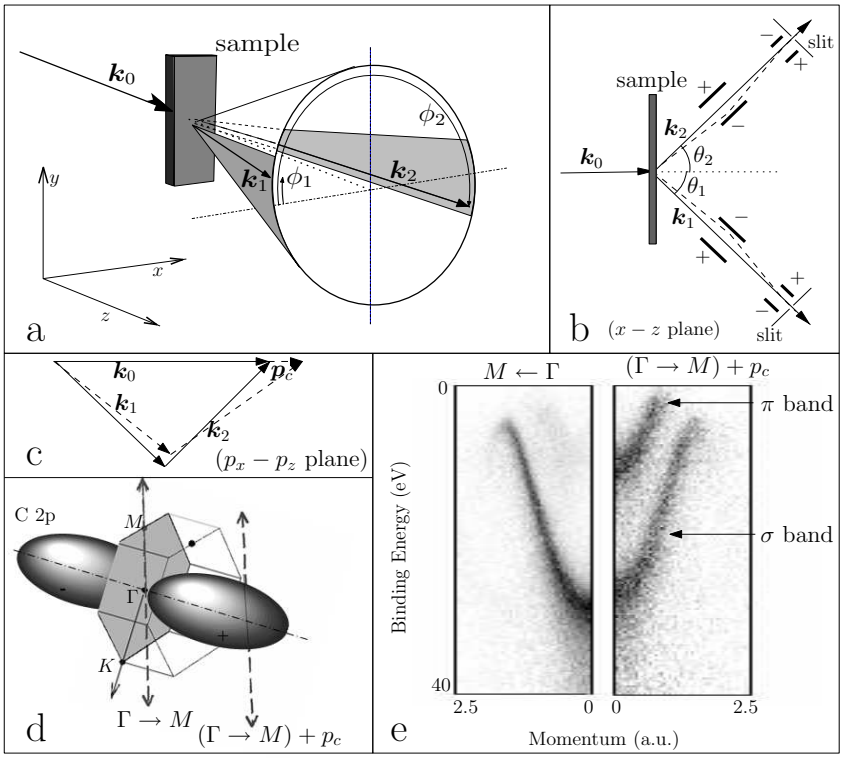

Figure 1: (a) Sketch of the EMS spectrometer. Electrons that emerge from the sample in the shaded part of the cone are detected. (b) An illustration of the use of deflectors for changing the scattering angles. Without deflector voltages the trajectories drawn as a full line are entering the analyzer through the slits, with voltages those drawn as a dashed line are entering. (c) The analyzers are positioned such that one measures electrons with no momentum in the p_x-p_y plane if one does not apply voltages to the deflectors. By applying equal voltages and polarities as shown in (b), we can measure target electrons with a momentum component along the p_z-axis. (d) For graphite the 2p electrons perpendicular to the graphite plane retain much of their atomic character and form the π band. The momentum space wave function is sketched together with the first Brillouin zone. (e) For the measurement without voltages on the delectors the intensity of the π electrons is absent (left), but its contribution appears if the deflectors are used (right), which moves the measurement line from Γ→M to (Γ→M)+p_c.

has $k_1 \sin\theta_1 \cos\phi_1 \approx -k_2 \sin\theta_2 \cos\phi_2$ (i.e. $q_x = 0$) but $k_1 \cos\theta_1 + k_2 \cos\theta_2 > k_0$, hence coincidences are expected for target electrons with $q_z > 0$.

The dramatic effect of orientation of the orbitals is best illustrated for the case of graphite. Graphite is a layered material, with strong covalent bonding in the hexagonal planes (giving rise to the "σ band"), but weak van der Waals bonding in between the planes. One 2p orbital (in coordinate space) is oriented perpendicular to the hexagonal planes, it forms the π band in graphite, and its wave function changes sign when crossing this plane. Hence the density is zero at the hexagonal plane. The graphite sample is positioned in the spectrometer with the *z*-axis along the surface normal of the hexagonal planes [9]. In momentum space this wave function changes sign relative to the q_z=0 plane and hence the momentum density is 0 here. Thus no coincidences are expected from the π band for $\theta_1 = \theta_2 = 44.3^\circ$, but the π band should contribute if deflector voltages are applied. This is indeed the case, as can be seen in the last panel of Fig. 1.

Brillouin zone boundaries play an important role in the theory describing the electronic structure of crystalline materials. It can be defined as the plane in momentum space, containing vectors **k** for which $2\mathbf{k}\cdot\mathbf{G} = G^2$, with **G** a reciprocal lattice vector [10]. Its role is best illustrated starting with a free electron model and treating the lattice potential as a perturbation. The solution of the free electron model consists of plane waves, and the perturbation (crystal potential V) is periodic and can be written as $V(\mathbf{r}) = \Sigma V_{\mathbf{G}} e^{i\mathbf{G}\cdot\mathbf{r}}$ with the sum extending over all reciprocal lattice vectors. From the definition of the reciprocal lattice vector it is clear that for each plane wave with momentum vector **q** on a Brillouin zone boundary there is another momentum vector (**q** - **G**) that has the same kinetic energy. These two states are degenerate and will thus split due to the interaction V_G.

This basic physics is illustrated in figure 2 for a silicon crystal with <001> surface normal. Details are given elsewhere [11]. The measurements were done without deflector voltages (hence one observes coincidences from electrons with $q_z = q_x = 0$). First the crystal was oriented so that the spectrometer *y*-axis coincides with a <110> direction of the crystal. Then the crystal was rotated, in several steps, along the surface normal until a <100> axis coincides with the *y*-axis. Thus first one observes the electrons moving along the <110> direction, and finally the electrons moving along the <100> direction. Two type_of Brillouinzone boundaries come into play. One is derived from G= $(\bar{2}00)$ and the other is a crossing_of two boundaries that are not perpendicular to the cut of fig. 2 (G= $(\bar{1}\,\bar{1}\,1)$ and G= $(\bar{1}\,\bar{1}\,1)$). However, V_{200}=0 due to additional symmetry in the crystal. Hence one only expects splitting of the intensity near the latter Brillouin zone boundary.

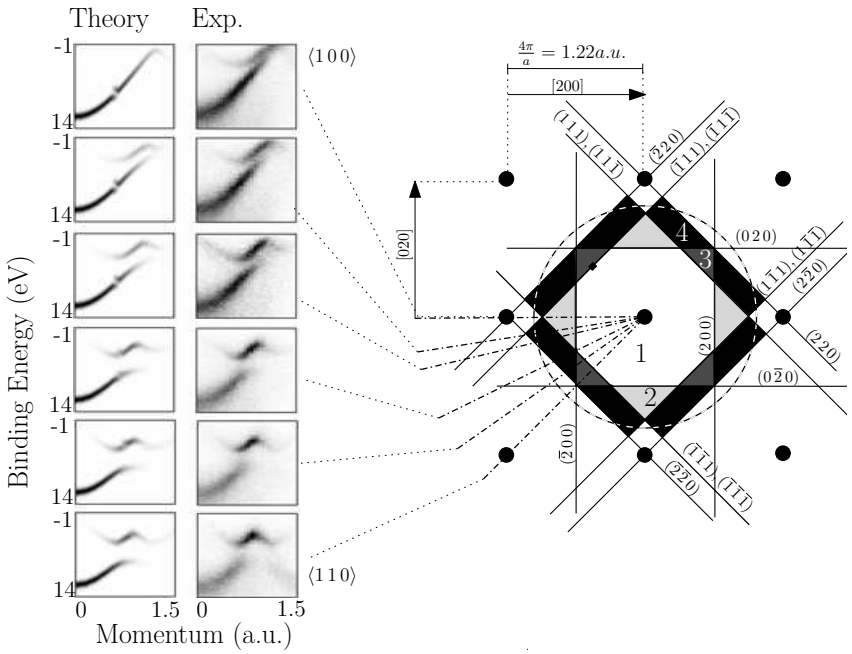

Figure 2: Measured intensities for a silicon single crystal as a function of orientation. The leftmost set of grey-scale pictures displays the calculated spectral function along different directions. These calculations are based on the FP-LMTO (full-potential linear muffin tin orbital) approach. Darker shades mean larger densities. The right column of grey-scale pictures are the corresponding experimental measurements. In the right half of the drawing we show the *<100> -<010>* plane of the reciprocal lattice with the first 4 Brillouin zones. By rotating the crystal one can change the crystallographic direction that coincides with the spectrometer *y*-direction. The actual measurement directions are indicated by dashed lines. Brillouin zone boundaries are marked with the indices of the reciprocal lattice vector they dissect. A band gap appears for momenta where the measurement line intersects the (111) and (111) Brillouin zone boundary. This splitting moves to lower momentum values when the measurement direction is changed from <100> to <110>. The dashed circle is the Fermi sphere for an electron gas with the same electron density as the valence band of Si. Occupation outside this sphere is small.

Indeed along the <110> direction the splitting is near q_y=0.6 a.u. Here two Brillouin zone boundaries are crossed ($(\bar{1}\,\bar{1}\,1)$ and $(1\,1\,1)$ and hence the occupation goes from band 1 to band 3. This measurement line crosses another Brillouin zone (corresponding to $(\bar{2}\bar{2}0)$) near 0.9 a.u. This is evident from a minimum in binding energy at this momentum. The band gap here separates the occupied and unoccupied part of the band structure. Hence the next bands (band 5 and 6) are not observed. Rotating the crystal in steps from <110> to <100> causes a shift of the first band gap to higher momentum values. Finally for the <100> direction the theory predicts only one structure, whereas two structures are seen for small binding energies. Due to finite momentum resolution the experiment probes part of Brillouin zone 4 abutting the measurement line, causing the extra structure.

Another central concept in band structure theory is that of the Bloch function. As the potential is periodic, its Fourier transform contains only discrete contributions, separated by reciprocal lattice vectors. As a consequence the solution of the Schrödinger equation (called Bloch functions) consists of a set of plane waves that differ by a reciprocal lattice vector. A solution can then be characterized by the reduced momentum k, the momentum of the component in the first Brillouin zone that contributes to Bloch function [10]. The Bloch function is a sum of plane waves, with amplitude $c_{\mathbf{G}}$:

$$\psi_{\mathbf{k}} = \sum_{\mathbf{G}} c_{\mathbf{G}} e^{i(\mathbf{k}+\mathbf{G})\cdot\mathbf{r}} .$$

Within this picture it is often stated that two momenta, which differ by a reciprocal lattice vector, correspond to the same reduced momentum and are considered equivalent. We explored what this means experimentally by measuring the spectral momentum density along lines that differ by a reciprocal lattice vector [12]. This can again be accomplished using the deflectors. For this purpose one applies different potentials to both deflectors. The experiment is sketched in fig. 3. Again silicon is used to demonstrate these principles. The crystal is aligned with the <110> direction along the y-axis. The deflectors can be used to create any momentum offset in the p_x-p_z plane. Without deflector voltages the measurement line goes through zero momentum, a reciprocal lattice point also referred to as a Γ point. This is the same measurement as in the lower panel of fig. 2. The shortest reciprocal lattice vector is (111). Applying an offset corresponding to (001) (itself *not* a reciprocal lattice vector) causes a shift of the measurement line so it goes again through reciprocal lattice points (at (111) and at $(\bar{1}\,\bar{1}\,1)$) (central panel of fig. 3).

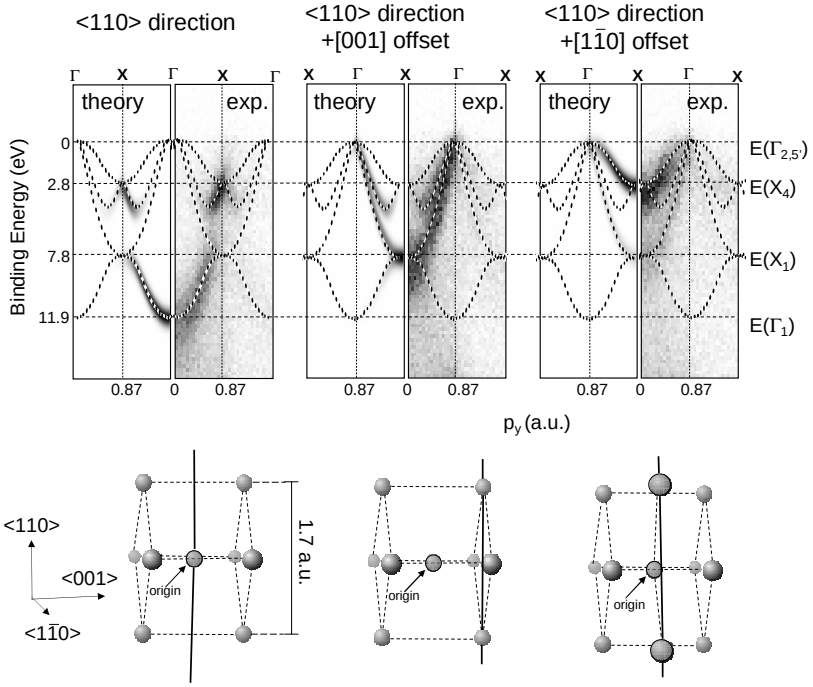

Figure 3: Calculated and observed intensities for a Si crystal measured with the <110> direction aligned with the spectrometer *y*-axis without the use of the deflectors (left panel, measuring along a line through zero momentum) and with voltages applied to the deflectors, in such a way that the measurement lines are shifted by [001] (central panel) and [1$\bar{1}$0] (right panel). As is indicated in the lower half, each of the three measurement lines goes through reciprocal lattice points, and one measurement line can be obtained from another by a shift corresponding to a reciprocal lattice vector. The calculated band structure is superimposed on the calculated and measured intensity distributions in such a way that Γ points of the band structure coincides with reciprocal lattice points. For all three cases the experiment shows significant intensity only at binding energies corresponding to the calculated bands. Which band is observed is different however, for all three cases, both in experimentally and theoretically obtained. momentum densities.

Alternatively the deflectors can be used to create a $(1\bar{1}0)$ offset, and one measures the spectra at a reciprocal lattice point (200) or $(2\bar{2}0)$ (right panel of figure 3). As these points are all separated by reciprocal lattice vectors it means that they are 'equivalent' with (000). Does this mean that the spectra measured that (000), (111) and (200) are identical? Inspection of figure 3 reveals that this is not the case. At the Γ point there are two (occupied) solutions with different energies. The solution with maximum binding energy dominates the spectrum at (000) the other solution (minimum binding energy) dominates the spectrum at (111) and (200).

To emphasize the Bloch theorem the band structure is superimposed, in the repeated zone scheme, on the measured intensity. Except for the high symmetry points, Γ and X, the band structure predicts 4 possible energies. Indeed the observed intensities always coincide with the energies predicted by the band structure. However, which branch of the band structure dominates, depends on the offset. The observed intensity is proportional to $|c_G|^2$ the modulus square of the coefficients of the Bloch function.

Finally, to illustrate that these measurements are possible as well for targets of heavier elements, we show in figure 4 the measured intensity for the noble metals along the three main symmetry directions. All noble metals have an FCC crystal structure with comparable lattice constants. As a consequence the electronic structures of the three noble metals share many features. Near zero momentum a parabolic shape is observed. It is due to the s electrons. At larger momenta we observe more weakly dispersing features due to the d electrons. But there are also clear differences between the three metals. For Ag the 4d intensity is at larger binding energy compared to the 3d intensity of Cu For Au the 5d intensity is split in different bands due to spin-orbit coupling. With increasing atomic number *Z* one also observes an increasing amount of diffraction. Diffraction causes the momentum of the incoming or outgoing electron to change by a reciprocal lattice vector. A tell-tale sign of this is a ghost-image of the s electron-derived parabola at higher momentum. Disentangling this contribution from the electronic structure proper is a problem that is currently being investigated.

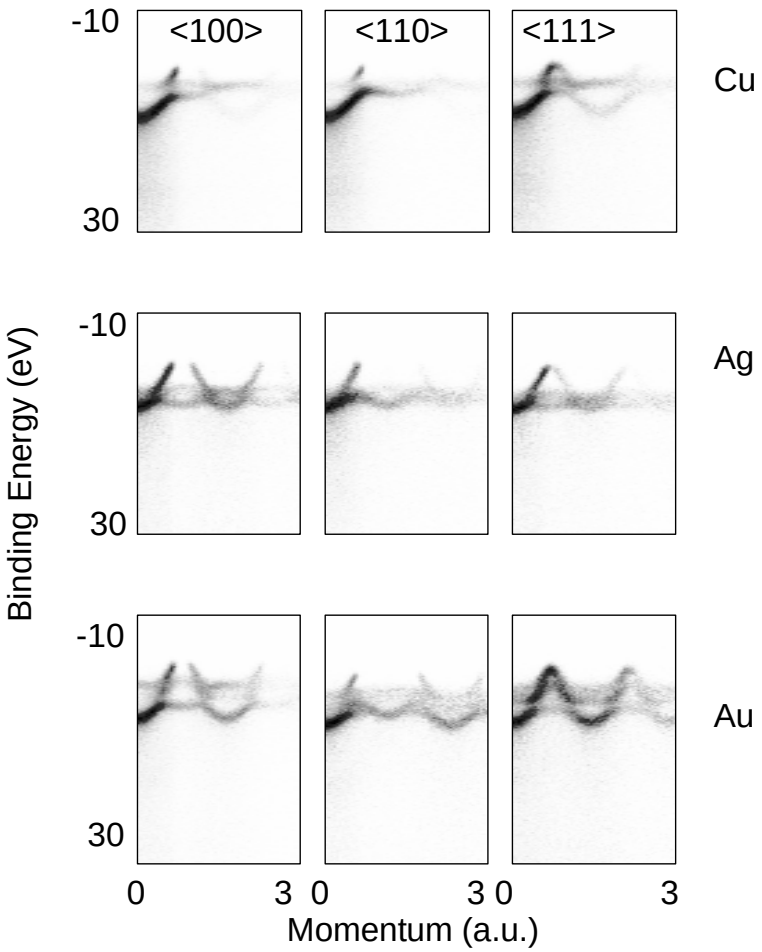

Figure 4: The measured intensity for Cu (top), Ag (middle) and Au (bottom) single crystal films, for crystals aligned with the <100> (left row), <110> (central row) and <111> direction. Similarities are due to the fact that the noble metals have the same lattice structure, similar lattice constants and the same number of valence electrons. The horizontal branches are due to d electrons and the parabola due to the s electrons. Diffraction causes a repeat of the main features at higher momentum. The increasing influence of diffraction with increasing *Z* is clearly noticeable.

Conclusion

We have shown that for single crystals we can obtain EMS results that are not affected by spherical averaging. This makes it possible to explore directly the anisotropy of the electronic structure. We demonstrated this capability by measuring the orientation of the π electrons in graphite and by determining the effect of rotation of the crystal for silicon. Also for silicon we studied the electronic structure along lines that differ by a reciprocal lattice vector. These measurements are clear illustrations of concepts such as Brillouin zone boundaries and Bloch functions.

These results are just one more example that kinematically complete collision experiments can provide very direct information of the structure of matter. It was made possible due to efforts of many collaborators, first at Flinders University, and more recently at the Australian National University. Ian McCarthy was pivotal in establishing the theoretical frame work that justified the simple interpretation of these experiments. These collision experiments will undoubtedly continue to be refined, increasing its value as a tool to elucidate the structure of matter. This guarantees that the impact of Ian's work will persist for quite some time to come.

Acknowledgements

The author wishes to thank Cameron Bowles, Erich Weigold and Michael Went for critically reading the manuscript. The research was made possible by funding of the Australian Research Council.

References

[1] P. E. Sokol, R. N. Silver and J. W. Clark, eds., *Momentum distributions* (1989).
[2] K. L. Lim and I. E. McCarthy, Phys. Rev. Lett. **13**(14), 446 (1964).
[3] E. Weigold and I. E. McCarthy, *Electron Momentum Spectroscopy* (Kluwer Academic/Plenum, New York, 1999).
[4] M. Takahashi, N. Watanabe, Y. Khajuria, Y. Udagawa and J. H. D. Eland, Phys. Rev. Lett. **94** (21), 213202 (2005).
[5] V. G. Neudatchin, Y. V. Popov and Y. F. Smirnov, Sov. Phys. Usp. **42**, 1017 (1999).
[6] C. Gao, A. L. Ritter, J. R. Dennison and N. A. W. Holzwarth, Phys. Rev. B **37**, 3914 (1988).
[7] P. Storer, R. S. Caprari, S. A. C. Clark, M. Vos and E. Weigold, Rev. Sci. Instrum. **65**, 2214 (1994).
[8] M. Vos, G. P. Cornish and E. Weigold, Rev. Sci. Instrum. **71**, 3831 (2000).
[9] E. Weigold, A.S. Kheifets, V.A. Sashin and M. Vos, Acta Cryst **A60**, 104 (2004).
[10] C. Kittel, *Introduction to Solid State Physics, 6th edition* (Wiley, New York, 1986).
[11] C. Bowles, A. Kheifets, V. Sashin, M. Vos and E. Weigold, J. Elec. Spec. Relat. Phenom. **141**, 95 (2004).
[12] M. Vos, C. Bowles, A. S. Kheifets and M. R. Went, Phys. Rev. B **73**, 085207 (2006).